

The Creation of Electrospun Nanofibers from Platelet Rich Plasma

Patricia S Wolfe^{1#}, Scott A Sell^{1,2#}, Jeffery J Ericksen^{2,3}, David G Simpson⁴ and Gary L Bowlin^{1*}

¹Department of Biomedical Engineering, Virginia Commonwealth University, 401 W. Main St., Richmond, VA 23284, USA

²Physical Medicine and Rehabilitation Service, Hunter Holmes McGuire VA Medical Center, 1201 Broad Rock Blvd., Richmond, VA 23249, USA

³Department of Physical Medicine and Rehabilitation, Virginia Commonwealth University, Richmond, VA 23298, USA

⁴Department of Anatomy and Neurobiology, Virginia Commonwealth University, Richmond, VA 23298, USA

*Authors contributed equally

Abstract

Activated platelet rich plasma (a PRP) contains supra physiologic amounts of autologous growth factors and cytokines known to enhance wound healing and tissue regeneration. Here we report the first results of electro spinning nanofibers from a PRP to create fibrous scaffolds that could be used for various tissue engineering applications. Human platelet rich plasma (PRP) was created, activated by a freeze-thaw-freeze process, and lyophilized to form a powdered preparation rich in growth factors (PRGF). It was dissolved in 1,1,1,3,3,3-hexafluoro-2-propanol (HFP) at different concentrations to form fibers with average diameters of 0.3 – 3.6 μm . A sustained release of protein from the PRGF scaffolds was demonstrated up to 35 days, and cell interactions with the PRGF scaffolds confirmed cell infiltration after just 3 days. As electro spinning is a simple process, and PRGF contains naturally occurring growth factors in physiologic ratios, creating nanofibrous structures from PRGF has the potential to be beneficial for a variety of tissue engineering applications.

Keywords: Platelet-rich plasma; Electro spinning; Tissue engineering; Scaffold; ECM

Introduction

The creation of tissue engineering scaffolds through the process of electrospinning has yielded promising results for the field of regenerative medicine over the last decade. These scaffolds can replicate the sub-micron scale topography of the native extracellular matrix (ECM), through the creation of nanoscale, non-woven fibers, using a number of natural and synthetic polymers. Using the process of electrospinning it is also possible to control the alignment and orientation of the created fibers, creating scaffolds that can be easily customized for nearly any tissue in the body. This control over fiber orientation, coupled with the diverse array of polymers conducive to being electrospun, allows for the tissue engineer to create structures with tailorable mechanical properties. Additionally, these scaffolds exhibit high surface area-to-volume ratios, high porosities, and variable pore-size distributions that mimic the native ECM and effectively create a dynamic structure capable of sustaining the passive transport of nutrients and waste throughout the structures [1-7].

However, despite the porosity and flexibility afforded by the electrospinning process, it is still considered to be quite challenging to promote cellular penetration into the depth of an electrospun structure, with cells preferring to proliferate and migrate across the surface of the scaffold rather than venture inside it [8-11]. While a number of rather novel techniques have been employed to increase cellularization of electrospun scaffolds [9,11,12], nothing has been proven to be ideal, nor to date become common practice in the field. The incorporation of growth factors into electrospun matrices for tissue engineering has the potential to enhance scaffold bioactivity, by supplying appropriate physical and chemical cues to promote cellular proliferation and migration, thereby increasing the cellularization of the structures [1,13,14]. By replicating the role of the native ECM in the normal wound healing cascade, that is serving as a reservoir of soluble growth factors critical to regeneration and providing a template for tissue repair, it may be possible to accelerate cellularization and tissue repair [3,13].

Platelet-rich plasma (PRP) is a supraphysiologic concentration of platelets suspended in plasma intended to serve as an autologous source of concentrated growth factors and cytokines. The use of PRP has been growing rapidly in the clinical world, as activated-PRP (aPRP) has been proven effective in accelerating healing in a number of tissues: osteochondral defects [15-17], tendon/ligament injuries [15-21], and chronic skin wounds (diabetic and pressure ulcers) [16,17,22,23]. The creation of a PRP is a relatively simple procedure that can be performed bedside, typically involving a blood draw and centrifugation to concentrate the platelet portion, followed by a platelet activation step and the delivery of the a PRP to the site of injury. There have been several methods reported in the literature on successfully activating and delivering a PRP to an injury site, with most involving the creation of a platelet gel using thrombin [15-17,24] or CaCl_2 [15-17,25]. These a PRP gels can then be easily applied to wound sites through injection or topical application.

The basis behind the use of these aPRP gels is that through the activation of the platelets, the alpha and dense granules contained within the platelets release an array of growth factors and cytokines critical to mediating normal wound healing [15,17,25-27]. The milieu of growth factors and cytokines released from the a PRP are in physiologically relevant ratios, albeit in concentrations several times higher than that of normal blood due to the linear relationship between platelet and growth factors concentrations [28]. Activated PRP has been shown to contain platelet derived growth factor (PDGF), transforming growth factor- β (TGF- β), vascular endothelial growth

*Corresponding author: Dr. Gary L. Bowlin, Department of Biomedical Engineering, Virginia Commonwealth University, P.O. Box 843067, Richmond, VA 23284, Email: gbowlin@vcu.edu

Received March 08, 2011; Accepted May 18, 2011; Published May 20, 2011

Citation: Wolfe PS, Sell SA, Ericksen JJ, Simpson DG, Bowlin GL (2011) The Creation of Electrospun Nanofibers from Platelet Rich Plasma. J Tissue Sci Eng 2:107. doi:10.4172/2157-7552.1000107

Copyright: © 2011 Wolfe PS, et al. This is an open-access article distributed under the terms of the Creative Commons Attribution License, which permits unrestricted use, distribution, and reproduction in any medium, provided the original author and source are credited.

factor (VEGF), fibroblast growth factor (FGF), epidermal growth factor (EGF), and others in elevated concentrations [15,17,18,22, 25-27]. Activated PRP has also been shown to contain a number of macrophage and monocyte mediators such as RANTES (Regulated upon Activation, Normal T-cell Expressed, and Secreted), lipoxin, and an array of interleukins capable of mediating inflammation [26]. In addition, the plasma portion of the PRP contains the proteins albumin, fibrinogen, a number of immunoglobulins, and more [29-31].

While the incorporation of growth factors and cytokines into electrospun scaffolds to modify cellular response is not new, the majority of studies have previously investigated single or multiple growth factors from isolated or recombinant sources. This method can be prohibitively expensive and difficult to deliver physiologically relevant concentrations [14,15,32], while aPRP has proven an efficient and cost-effective method for acquiring a number of highly concentrated factors. The purpose of this study was to create an electro spun scaffold that would harness the reparative potential and bioactivity found in a PRP, namely the growth factor and cytokine milieu contained within, by lyophilizing a PRP and creating PRGF suitable for electro spinning. Utilizing the plasma proteins contained within the PRGF, namely fibrinogen which has been successfully electrospun in the past [33-36], it was hypothesized that pure lyophilized PRGF could be electro spun into a stable scaffolding material for tissue engineering applications. Such a scaffold, containing a concentration of multiple growth factors and cytokines, would have the potential to promote cellularization of the structure while providing a sustained release of growth factors capable of providing a chemotactic gradient for cellular recruitment.

Methods

Creation of aPRP and PRGF

Fresh human whole blood from 3 donors was purchased (Biological Specialty Corp., Colmar, PA, USA), pooled, and used in a SmartPREP² (Harvest Technologies Corp., Plymouth, MA, USA) centrifugation system to create PRP per manufacturers protocol. A small aliquot of both pooled whole blood and PRP were sent to the Harvard Immune Disease Institute's Blood Research laboratory to determine their respective platelet concentrations. PRP was then subjected to a freeze-thaw-freeze (FTF) cycle for platelet lysis and activation. Briefly, PRP was placed in a -70° C freezer for 24 hrs followed by a 37° C waterbath for 1 hr, and then returned to the -70° C freezer for 24 hrs. This method has previously been found to contain the same, and in some cases, higher levels of bFGF and VEGF as thrombin and CaCl₂ aPRP (data not published). Frozen aPRP was then lyophilized for 24 hrs to create a dry PRGF powder which was finely ground in a mortar and pestle prior to use.

Creation of electrospun PRGF scaffolds

PRGF was dissolved in 1,1,1,3,3,3-hexafluoro-2-propanol (HFP, TCI America Inc., Portland, OR, USA) at different concentrations, ranging from 80-280 mg/ml, to determine the optimum fiber forming concentration range. HFP was used as the solvent because, not only is it the most widely used solvent in our lab, but it also is very versatile in creating nanofibrous scaffolds from a variety of natural and synthetic polymers without much difficulty. In addition, previously published studies performed by our lab, as well as many others, have shown electrospun scaffolds fabricated from HFP are biocompatible [11,33,37-42]. Once in solution, PRGF was loaded into a 3 mL Becton Dickinson syringe, and placed in a KD Scientific syringe pump (model number 100, Holliston, MA, USA) for dispensing at a rate of 2.5 ml/

hr. A blunt 18 gauge needle was placed on the syringe, and the positive voltage lead of a power supply (Spellman CZE1000R; Spellman High Voltage Electronics Corp., Hauppauge, NY, USA) was attached to the needle and set to 25 kV. A grounded mandrel (1.9 cm wide x 7.6 cm long x 0.5 cm thick; 303 stainless steel) was placed 15 cm away from the needle tip and was rotated at 500 rpm and translated at 7.5 cm/s over 15 cm distance for collection of the fibers.

Electrospun scaffold characterization

Scanning electron micrographs and fiber diameter: Fiber diameter characterization was accomplished using scanning electron micrographs (SEM, Zeiss EVO 50 XVP, Peabody, MA, USA) of each scaffold. Samples from each scaffold were mounted on an aluminum stub and sputter coated with gold for imaging. The average fiber diameter of each electrospun structure was determined from the SEM images using UTHSCSA ImageTool 3.0 software (Shareware provided by University of Texas Health Science Center in San Antonio). Fiber diameter averages and standard deviations were calculated by taking the average of 60 random measurements per micrograph.

Protein release kinetics: From scaffolds of 100, 150, and 200 mg/ml PRGF, 10 mm diameter discs were punched, disinfected with a 30 minute soak in ethanol, followed by three 10 minute rinses in PBS, and placed in a 48 well plate with 500 µl of PBS. On days 1, 4, 7, 10, 14, 21, 28 and 35, PBS was retained and kept in a -70 °C until ready for evaluation. A generic protein assay (BCA Protein Assay, Thermo Scientific Pierce, Rockford, IL, USA) was performed on samples to quantify the concentration of total protein released from the PRGF scaffolds.

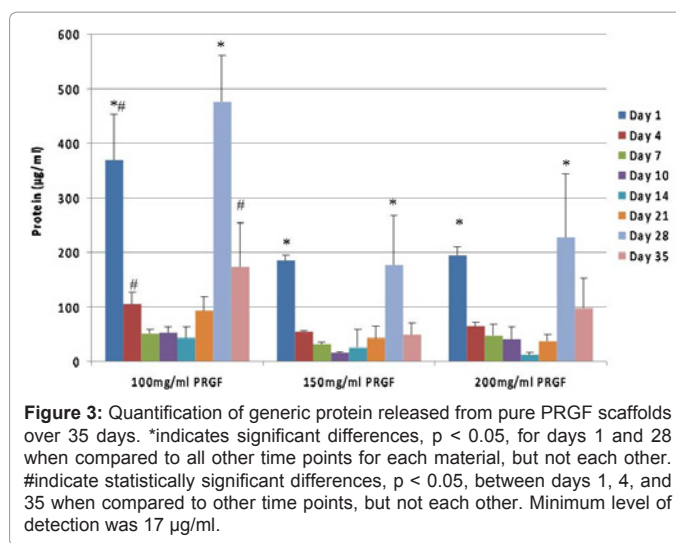
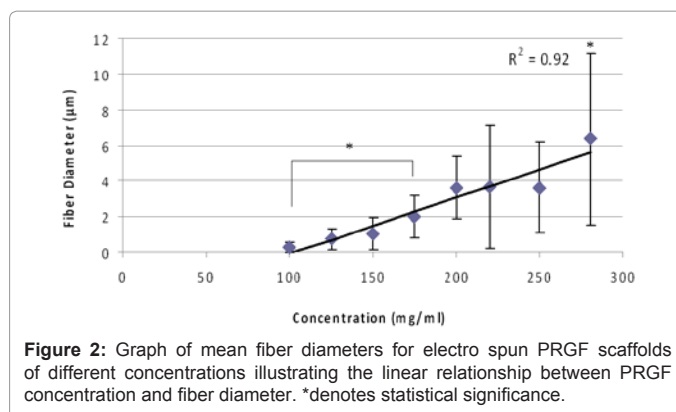
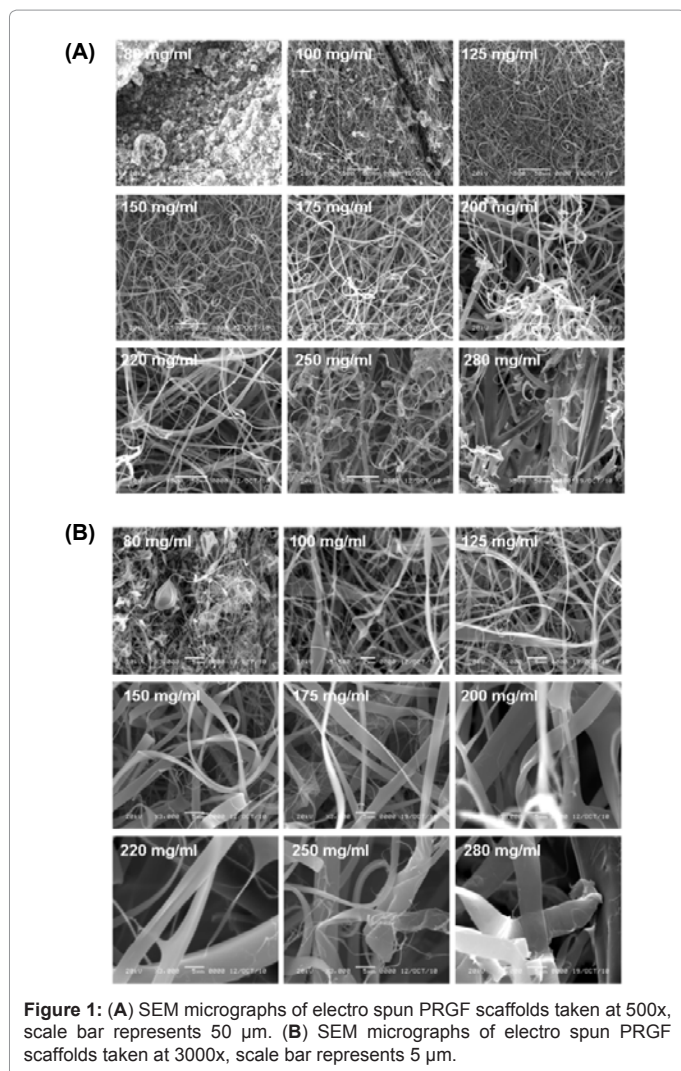
Gel electrophoresis: Gel electrophoresis was performed to analyze the molecular weight of the proteins in PRGF, platelet poor plasma (PPP), and electrospun PRGF scaffolds and compare them to those of fibrinogen (FBG, Sigma Aldrich, St. Louis, MO, USA) and bovine serum albumin (BSA, Sigma Aldrich, St. Louis, MO, USA) controls. Briefly, 2 mg BSA, FBG, PRGF, and 100, 150, 200 mg/ml PRGF scaffolds were solubilized in a reducing agent containing laemmli buffer with 5 % β-mercaptoethanol. Samples were boiled for 3-5 minutes to further ensure they were solubilized, and 10 µL of each sample was placed in duplicate in each lane of 4-15% polyacrylamide 18-well gels (Criterion Bio-Rad, Hercules, CA, USA). A molecular weight protein ladder (20 µL, Sigma Aldrich, St. Louis, MO, USA) was run to provide a molecular weight basis for protein identification and comparison. Samples were run at constant voltage of 120 V over 2 hours. After the 2 hours, the gels were stained with Coomassie Blue, and evaluated by the Bio-Rad Gel DocTM 2000 system.

Fluorescent based assay: FBG concentration was quantified in the PRGF electrospun scaffolds, as well as in aPRP, blood and PPP by using a fluorescent based assay. Scaffolds of 100, 150, and 200 mg/ml electrospun PRGF (10 mm diameter discs, n=4) were placed in a 48 well plate and blocked with Odyssey Blocking Buffer (LI-COR Biosciences, Lincoln, NE, USA) for 1 hour at room temperature. Simultaneously, human FBG from reference plasma (Fisher Scientific, Pittsburgh, PA, USA) was diluted in DI water at concentrations of 76, 38, 19, 9.5, 4.75, 2.38, 1.19, 0.59, and 0 mg/dl and was blotted on a PVDF membrane, along with a PRP, PPP, blood, and PRGF diluted in water at 10, 5, and 1 mg/ml. The membrane was blocked in Odyssey Blocking Buffer for one hour at room temperature. After blocking, standards and samples were incubated in anti-human fibrinogen antibody (Millipore, Billerica, MA, USA) at room temperature for 1.5 hours. All samples and standards were then washed four times with 0.1% Tween-20 in PBS, after which the signal from mouse anti-human fibrinogen antibody was detected

with goat anti-mouse IgG secondary antibody tagged with a fluorescent 800 nm marker (Thermo Scientific, Pittsburgh, PA, USA). To account for antibody background fluorescence, each scaffold was incubated with secondary antibody only. Samples and standards were incubated in the secondary antibody for 1 hour at room temperature without exposure to light. After washing, the samples were scanned using the 800 nm channel of the Odyssey Infrared Imaging System (LI-COR Biosciences, Lincoln, NE) at an intensity of 3.5. Fluorescence intensities were measured using circular gates that completely surrounded the scaffolds and well plates. Background fluorescence that was obtained from samples incubated with secondary antibody only was subtracted from the signal intensities of the samples incubated with both primary and secondary antibodies.

Evaluation of cell interaction

To determine the interaction of human cells on electrospun PRGF scaffolds, 10 mm diameter discs were punched from scaffolds of 100, 150, and 200 mg/ml PRGF, disinfected (30 minute soak in ethanol followed by three 10 minute rinses in PBS), and placed in a 48 well plate. A sterile Pyrex cloning ring (10 mm outer diameter, 8 mm inner diameter) was placed on top of each scaffold to prevent them from floating, and to ensure all cells stayed on the surface of the scaffold during culture.



Each scaffold was seeded with either 100,000 human adipose derived stem cells (hADSC) isolated from medical waste lipoaspirate in 500 µl of complete media (DMEM low glucose supplemented with 10% FBS and 1% penicillin/streptomycin, Invitrogen, Carlsbad, CA, USA) or 100,000 human umbilical artery smooth muscle cells (hSMC, Lonza, Basel, Switzerland) in 500 µl of complete media (SMGM-2 bullet kit, Lonza, Basel, Switzerland). Controls consisted of scaffolds in complete media without cells. Media was changed every third day, and on days 3 and 10, scaffolds were fixed in 10% Formalin and cryosectioned for 4',6-diamidino-2-phenylindole (DAPI) staining.

Statistical analysis

Statistical analysis was performed using JMPIN 8.0 statistical software (SAS Institute, Inc., Cary, NC, USA) and was based on a Kruskal-Wallis one-way analysis of variance on ranks and a Tukey-Kramer pairwise multiple comparison procedure ($\alpha=0.5$). Graphical depictions of mean data were constructed with Microsoft Excel 2007, with error bars representing standard deviations.

Results and Discussion

Creation of a PRP and PRGF

It was determined by Harvard Immune Disease Institute's Blood Research Laboratory that the PRP created by the SmartPREP² centrifugation system resulted in a 5.5 fold increase in platelets compared to the pooled whole blood used in this study (955×10^3

platelets/ μl versus 175×10^3 platelets/ μl). This result is in agreement with published data [44], and based upon the linear relationship between platelet count and growth factor concentration, a resulting similar fold increase should present in platelet derived growth factor concentrations [28].

Electrospun scaffold characterization

SEM and fiber diameter: SEM characterization of the electrospun PRGF scaffolds is shown in Figure 1. The micrographs illustrate the nanofibrous structures of each scaffold starting around 100 mg/ml, with the appearance of a large range of fiber diameters for the different PRGF concentrations, as well as increased void space as PRGF concentration increases. Fiber diameters for the scaffolds range from $0.28 \pm 0.29 \mu\text{m}$ for 100 mg/ml PRGF to $6.37 \pm 4.81 \mu\text{m}$ for 280 mg/ml PRGF Figure 2. Statistical analysis reveals the average fiber diameters for 100 and 175 mg/ml PRGF are significantly different from all other scaffolds, with the exception of 125 and 150 mg/ml PRGF. Average fiber diameters for scaffolds of 200, 220, and 250 mg/ml PRGF are significantly different from all other scaffolds, but not each other. Scaffolds of 280 mg/ml PRGF have significantly greater fiber diameters from those of all other scaffolds. This linear relationship between polymer concentration and fiber diameter is expected, as it has been well established previously [2,36,37,40,45]. The broad range of fiber diameters produced during the electrospinning process allows for flexibility in the fabrication of electro spun scaffolds for different tissue engineering applications.

Protein release kinetics: The quantified protein release results from electrospun PRGF scaffolds are shown in Figure 3, demonstrating protein release from PRGF scaffolds was detectable over 35 days. The release kinetics illustrates a peak release of protein on day 1 for all scaffold concentrations, followed by a distinct decrease in release for days 4-21. Unexpectedly, at day 28, protein release increases for all scaffolds. By day 35 protein release has decreased, however, compared to days 4-21, overall release has increased. Surprisingly, 100 mg/ml PRGF scaffolds had the highest release of protein over the 35 days compared to the other scaffolds, releasing 370 $\mu\text{g}/\text{ml}$ of protein at day 1 and 175 $\mu\text{g}/\text{ml}$ by day 35. Scaffolds of 150 and 200 mg/ml PRGF had similar release kinetics over the 35 days (185 – 49 $\mu\text{g}/\text{ml}$ and 194 – 96 $\mu\text{g}/\text{ml}$ for the 150 and 200 mg/ml PRGF scaffolds, respectively). The initial burst release from scaffolds at day 1 is expected, as PRGF from the surface of the scaffolds is released. The high protein release from scaffolds of 100 mg/ml PRGF over the other scaffolds may be explained by the scaffold's smaller fiber diameters. Although not specifically investigated in this study, other previously published studies have demonstrated similar results, and explain that with smaller fiber diameters there is less distance for molecules to traverse to reach the fiber surface, hence, more protein release from the fibers over time [46-49]. The rise in protein release after day 21 may be due to fiber degradation of the PRGF scaffolds occurring around 28-35 days and subsequent release of entrapped proteins. Although degradation may have started to occur around day 28, the electro spun scaffolds were still very much intact at 35 days. This outcome was unexpected, as most electro spun natural polymers degrade rapidly in solution and need to be cross-linked or co-spun with a synthetic polymer to increase their stability [50]. Statistical analysis revealed protein release at day 1 and day 28 from all PRGF scaffolds was significantly greater than protein release from those respective scaffolds at all other time points (days 4, 7, 10, 14, 21, and 35). For scaffolds of 100 mg/ml PRGF, protein release at days 1, 4, and 35 was significantly different from that at all other time points for that respective scaffold (days 7, 10, 14, and 21).

Gel electrophoresis: The results from the gel electrophoresis technique are illustrated in Figure 4. The electrophoretic pattern of

FBG appears as expected, as it has been previously determined that the alpha, beta and gamma chains have average molecular weights of around 68, 58 and 50 kDa, respectively [51]. BSA also exhibits a pattern that would be expected, with a distinct band around 67 kDa [31,52,53]. The electrophoresis results of PRGF resembles those of BSA and the FBG alpha chain, with a distinct band around 68 kDa. This band is also likely to be representative of hemoglobin, which has a molecular weight of 68 kDa. PRGF also illustrates a faint band around 80 kDa, which is representative of different glycoproteins, including transferrin, and plasminogen, and a distinct thick band at 14 kDa, indicating the presence of multiple chains of haptoglobin and transthyretin [31]. These results are not surprising, due to the fact that plasma contains large amounts of these proteins. Interestingly, PPP has a similar electrophoretic pattern to that of both FBG and BSA, with the triple banding that is typically seen with FBG and the distinct band at 70 kDa that is characteristic of BSA. Additionally, PPP has additional banding around 80, 25, 18, and other faint bands between 25 – 50 kDa. These bands most likely represent a multitude of components, including different kinds of glycoproteins (similar to PRGF), various IgG light chains, multiple haptoglobin chains and various lipoproteins (both LDL and HDL) [31]. The fact that PPP is made up of mostly albumin, fibrinogen, and immunoglobulins is understandable, due to the fact that these components are the most prevalent proteins in blood.

Fluorescent based assay: The PVDF membrane that was spotted with 0 to 76 mg/dl of human FBG was scanned by the Odyssey system and fluorescent intensities were acquired. The standard curve obtained is shown in Figure 5, illustrating a linear relationship ($R^2 = 0.96$, $y =$

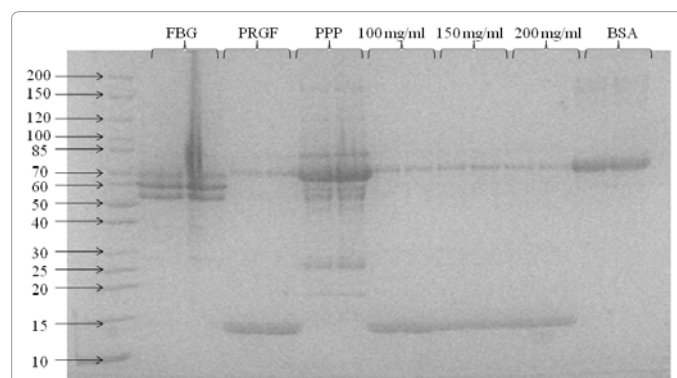


Figure 4: Electrophoretic patterns of molecular weight standards, FBG, PRGF, PPP, PRGF scaffolds of 100, 150, and 200 mg/ml and BSA in the 4-20% polyacrylamide gels.

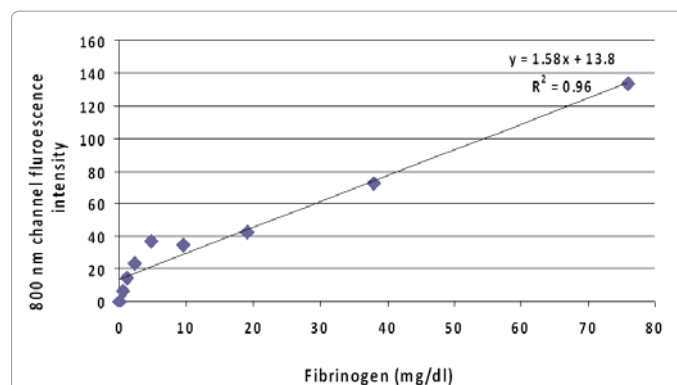


Figure 5: Linear curve ($R^2 = 0.96$) obtained from dilutions of human FBG standards for fluorescent assay.

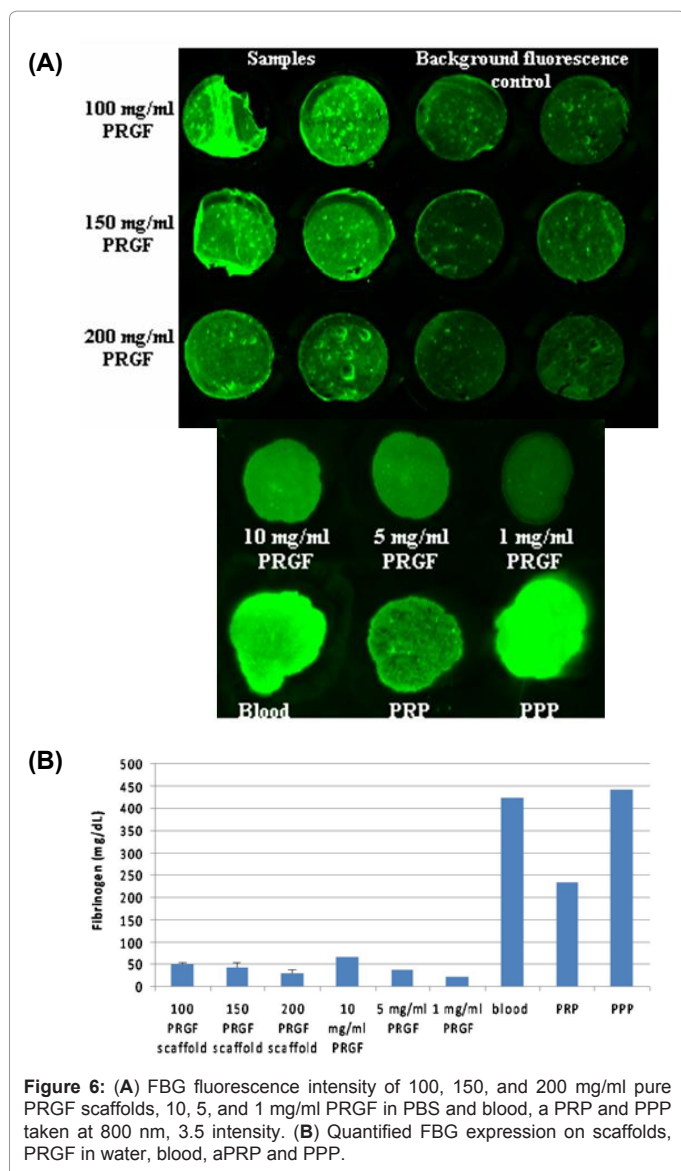


Figure 6: (A) FBG fluorescence intensity of 100, 150, and 200 mg/ml pure PRGF scaffolds, 10, 5, and 1 mg/ml PRGF in PBS and blood, a PRP and PPP taken at 800 nm, 3.5 intensity. (B) Quantified FBG expression on scaffolds, PRGF in water, blood, aPRP and PPP.

1.58x + 13.8). Using the standard curve equation, the amount of FBG in each sample was determined.

The amount of FBG expressed on scaffolds of pure PRGF ranged from 30-51 mg/dl (Figure 6, right). Specifically, 100 mg/ml PRGF amounted in 51 mg/dl FBG, 150 mg/ml PRGF contained 43 mg/dl FBG, and 200 mg/ml PRGF had 30 mg/dl FBG. PRGF diluted in water at 10, 5 and 1 mg/ml resulted in 67, 37, and 21 mg/dl FBG, respectively. Blood and PPP contained the highest amount of FBG (423 and 440 mg/dl, respectively), while aPRP contained only 234 mg/dl FBG. The values of FBG that were quantified in blood, aPRP, and PPP were expected, and are consistent with previously published data [44,54,55]. The reason behind why 200 mg/ml PRGF contained less amounts of FBG than 100 mg/ml PRGF is not completely understood, and will need to be investigated further in future studies.

The authors speculate the presence of FBG and hemoglobin in PRGF may be the reason why this protein is stable enough to form electro spun nanofibers. More specifically, Factor XIII, a stabilizing enzyme of the blood coagulation system that cross-links fibrin, may

explain why the electro spun PRGF scaffolds were still intact during the protein release study, even after 35 days in culture. This speculation is based on previous studies, which have demonstrated the ability of FBG and hemoglobin to form electro spun nanofibers from HFP [36,56]. In addition to the methods presented in this study, the presence of FBG, albumin, and hemoglobin in electrospun PRGF scaffolds was further confirmed by mass spectrometry.

Cell interaction: Results from DAPI staining of hADSCs cultured on pure PRGF scaffolds reveals cell penetration into the scaffolds after as little as 3 days (Figure 7). As PRGF electro spinning concentration increases from 100 to 200 mg/ml, it appears there is greater cell migration into the scaffolds, potentially due to the increase in average fiber diameter and subsequent increase in scaffold void space. Regardless, after 10 days it is evident hADSCs have migrated through the entire thickness of the PRGF scaffolds for all concentrations.

hSMC interaction with PRGF scaffolds is shown in Figure 8, demonstrating after only 3 days there is cell migration throughout the entire 200 mg/ml PRGF scaffold. 100 mg/ml PRGF scaffolds demonstrated little penetration of hSMCs into the scaffold, with most cells remaining on the surface of the scaffold even after 10 days. Scaffolds of 150 and 200 mg/ml PRGF had complete cellular migration throughout the entire scaffold by day 10. Surprisingly, hSMCs cultured on 150 mg/ml PRGF completely migrated from the surface of the scaffold into the middle region in only 10 days.

The reason for this rapid migration of cells into the scaffold may be two-fold: the presence of an array of chemokines and growth factors found in concentrated amounts in a PRP is most likely chemotactic towards multiple cell types, and the increased void space as PRGF

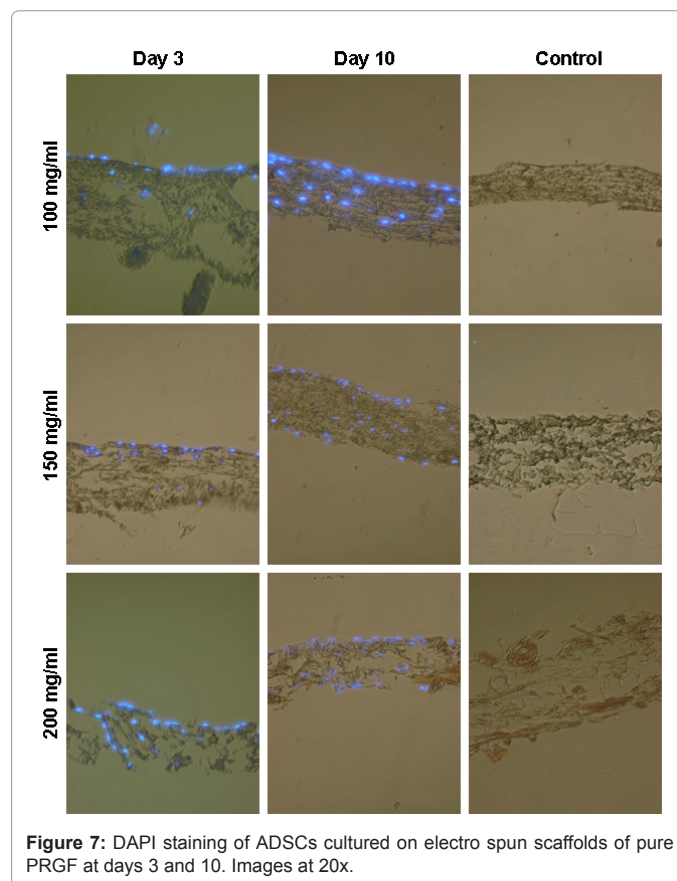


Figure 7: DAPI staining of ADSCs cultured on electro spun scaffolds of pure PRGF at days 3 and 10. Images at 20x.

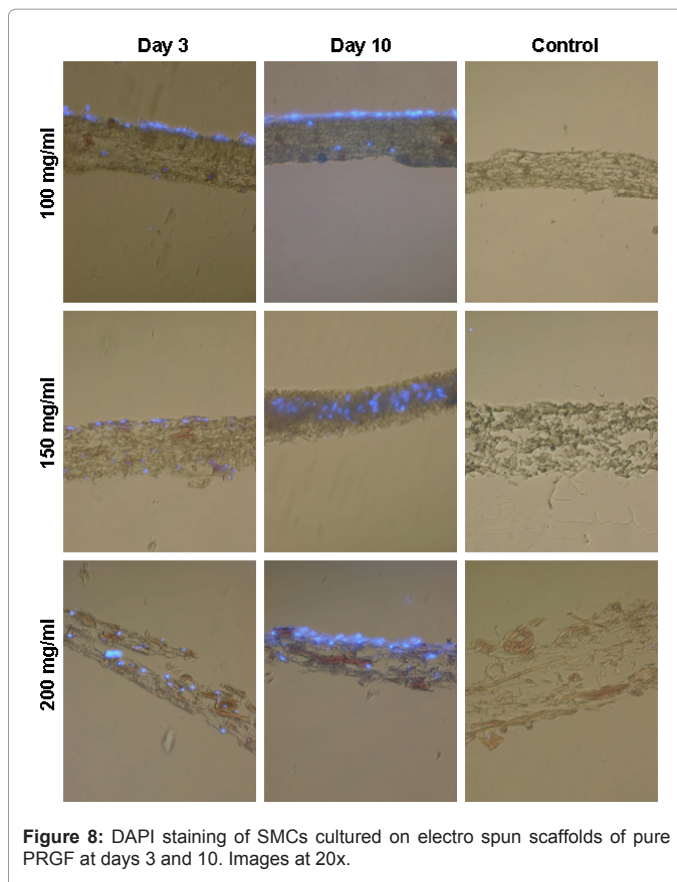


Figure 8: DAPI staining of SMCs cultured on electro spun scaffolds of pure PRGF at days 3 and 10. Images at 20x.

electro spinning concentration increases allows cells to easily migrate into the scaffold. Although not investigated in this manuscript, a previous study conducted by the authors has confirmed the release of RANTES and PDGF-bb from electro spun PRGF fibers (data not published). The release of these growth factors and cytokines, as well as many others contained within PRGF that have been previously shown to be chemotactic and induce cell proliferation, is most likely the reason for enhanced cell infiltration within the scaffolds. Although it was not directly analyzed in this study, from the SEMs it appears the difference in fiber diameters between the PRGF concentrations affects the porosity of the scaffolds, with increased void space occurring as PRGF concentration increases.

Conclusion

This manuscript demonstrates, for the first time, the feasibility of creating a nanofibrous scaffold from a PRP. As PRP has gained recent popularity in the clinical setting due to its ability to enhance healing and promote regeneration in an array of tissues clinically, it may prove beneficial when used as a tissue engineering scaffolding material. Not only did electro spun scaffolds of PRGF prove to be stable for extended periods of time in vitro, but they also exhibited a sustained release of proteins known to be important for tissue regeneration for up to 35 days. Additionally, despite the fact that electro spinning is often criticized for its perceived lack of cellular penetration, electro spun PRGF scaffolds promoted rapid cellular infiltration due to the presence of a milieu of growth and chemotactic factors inherent to a PRP. While this preliminary evaluation of electro spun PRGF demonstrated its tissue engineering potential in an in vitro setting, its true benefit may be seen in an in vivo scenario where multiple regenerative cell types can

act concomitantly on the scaffolds in a manner similar to the natural healing cascade through the sustained chemotactic and growth factor gradients eluted.

Acknowledgements

The authors would like to thank Drs. Sherwin Keyv and May Jacobsen from the Harvard Immune Disease Institute's Blood Research Laboratory for conducting platelet counts on pooled whole blood and PRP. The authors would also like to thank Dr. Kristina Nelson from the Virginia Commonwealth University Chemical and Proteomic Mass Spectrometry Core Facility for performing mass spectrometry on electro spun PRGF. Cryosectioning of PRGF scaffolds for DAPI staining was performed at the Virginia Commonwealth University Department of Anatomy and Neurobiology Microscopy Facility.

References

1. Kumbar, S.G, James R, Nukavarapu SP, Laurencin CT, et al. (2008) Electrospun nanofiber scaffolds: engineering soft tissues. *Biomed Mater*, 3: p.034002.
2. Barnes, C.P, Sell SA, Boland ED, Simpson DG, Bowlin GL (2007) Nanofiber technology: Designing the next generation of tissue engineering scaffolds. *Advanced Drug Delivery Reviews* 59:1413-1433.
3. Sell SA, Patricia SW, Garg K, McCool JM, Rodriguez IA, et al. (2010) The Use of Natural Polymers in Tissue Engineering: A Focus on Electrospun Extracellular Matrix Analogues. *Polymers* 2: 522-553.
4. Ramakrishna S, et al. (2005) Introduction to Electrospinning and Nanofibers: World Scientific Publishing Company, Incorporated.
5. Chew SY, Wen Y, Dzenis Y, Leong KW (2006) The role of electro spinning in the emerging field of nanomedicine. *Curr Pharm Des* 12: 4751-4770.
6. Lannutti J (2007) Electro spinning for tissue engineering scaffolds. *Mater Sci Eng C Biomimetic Supramol Syst* 27: 504-509.
7. Sill TJ, von Recum HA (2008) Electro spinning: applications in drug delivery and tissue engineering. *Biomaterials* 29: p. 1989-2006.
8. Nisbet DR, Forsythe JS, Shen W, Finkelstein DI, Home MK (2009) Review paper: a review of the cellular response on electrospun nanofibers for tissue engineering. *J Biomater Appl* 24: 7-29.
9. Baker BM, Gee AO, Metter RB, Nathan AS, Marklein RA, et al. (2008) The potential to improve cell infiltration in composite fiber-aligned electrospun scaffolds by the selective removal of sacrificial fibers. *Biomaterials* 29: 2348-2358.
10. Baker BM, Nerurkar NL, Burdick JA, Elliott DM, Mauck RL, et al. (2009) Fabrication and modeling of dynamic multipolymer nanofibrous scaffolds. *J Biomech Eng* 131: 101012.
11. Sell SA, McClure MJ, Ayres CE, Simpson DG, Bowlin GL (2010) Preliminary investigation of airgap electrospun silk fibroin-based structures for ligament analogue engineering. *J Biomater Sci Polym Ed In Press*.
12. Stankus JJ, Soletti L, Fujimoto K, Hong Y, Vorp DA, et al. (2007) Fabrication of cell microintegrated blood vessel constructs through electrohydrodynamic atomization. *Biomaterials* 28: 2738-2746.
13. Chen FM, Zhang M, Wu ZF (2010) Toward delivery of multiple growth factors in tissue engineering. *Biomaterials* 31: 6279-6308.
14. Sahoo S, Ang LT, Goh JC, Toh SL (2010) Growth factor delivery through electrospun nanofibers in scaffolds for tissue engineering applications. *J Biomed Mater Res A* 93: 1539-1550.
15. Foster TE, Puskas BL, Mandelbaum BR, Gerhardt MB, Rodeo SA (2009) Platelet-rich plasma: from basic science to clinical applications. *Am J Sports Med* 37: 2259-72.
16. Anitua E, Sánchez M, Orive G, Andia I (2008) Delivering growth factors for therapeutics. *Trends Pharmacol Sci* 29: 37-41.
17. Alsousou J, Thompson M, Hulley P, Noble A, Willett K (2009) The biology of platelet-rich plasma and its application in trauma and orthopaedic surgery: a review of the literature. *J Bone Joint Surg Br* 91: 987-996.
18. Creaney L and Hamilton B (2008) Growth factor delivery methods in the management of sports injuries: the state of play. *Br J Sports Med* 42: 314-320.
19. Lyras DN, Kazakos K, Verettas D, Botaitis S, Agrogiannis G, et al. (2009) The effect of platelet-rich plasma gel in the early phase of patellar tendon healing. *Arch Orthop Trauma Surg* 129: 1577-1582.

20. Murray MM, Spindler KP, Abreu E, Muller JA, Nedder A, et al. (2007) Collagen-platelet rich plasma hydrogel enhances primary repair of the porcine anterior cruciate ligament. *J Orthop Res* 25: 81-91.
21. Mishra A and Pavelko T (2006) Treatment of chronic elbow tendinosis with buffered platelet-rich plasma. *Am J Sports Med* 34: 1774-1778.
22. Rozman P, Bolta Z (2007) Use of platelet growth factors in treating wounds and soft-tissue injuries. *Acta Dermatovenerol Alp Panonica Adriat* 16: 156-65.
23. Anitua E, Aguirre JJ, Algorta J, Ayerdi E, Cabezas AI, et al. (2008) Effectiveness of autologous preparation rich in growth factors for the treatment of chronic cutaneous ulcers. *J Biomed Mater Res B Appl Biomater* 84: 415-421.
24. Kocaoemer A, Kern S, Klüter H, Bieback K (2007) Human AB serum and thrombin-activated platelet-rich plasma are suitable alternatives to fetal calf serum for the expansion of mesenchymal stem cells from adipose tissue. *Stem Cells* 25: 1270-1278.
25. Sanchez M, Anitua E, Orive G, Mujika I, Andia I (2009) Platelet-rich therapies in the treatment of orthopaedic sport injuries. *Sports Med* 39: 345-354.
26. El-Sharkawy H, Kantarci A, Deady J, Hasturk H, Liu H, et al. (2007) Platelet-rich plasma: growth factors and pro- and anti-inflammatory properties. *J Periodontol* 78: 661-669.
27. Everts PA, Knape JT, Weibrich G, Schönberger JP, Hoffmann J, et al. (2006) Platelet-rich plasma and platelet gel: a review. *J Extra Corpor Technol* 38: 174-187.
28. Jacobson M, Fufa D, Abreu EL, Kevy S, Murray MM (2008) Platelets, but not erythrocytes, significantly affect cytokine release and scaffold contraction in a provisional scaffold model. *Wound Repair Regen* 16: 370-378.
29. Jacobs JM, Adkins JN, Qian WJ, Liu T, Shen Y, et al. (2005) Utilizing human blood plasma for proteomic biomarker discovery. *J Proteome Res* 4:1073-1085.
30. Adkins JN, Varnum SM, Auberry KJ, Moore RJ, Angell NH, et al. (2002) Toward a human blood serum proteome: analysis by multidimensional separation coupled with mass spectrometry. *Mol Cell Proteomics* 1: 947-955.
31. Anderson L and Anderson NG (1977) High resolution two-dimensional electrophoresis of human plasma proteins. *Proc Natl Acad Sci USA* 74: 5421-5425.
32. Sahoo S, Toh SL, Goh JC (2010) A bFGF-releasing silk/PLGA-based biohybrid scaffold for ligament/tendon tissue engineering using mesenchymal progenitor cells. *Biomaterials* 31: 2990-2998.
33. McManus M, Boland E, Sell S, Bowen W, Koo H, et al. (2007) Electrospun nanofibre fibrinogen for urinary tract tissue reconstruction. *Biomedical Materials* 2: 257-262.
34. McManus MC, Boland ED, Koo HP, Barnes CP, Pawlowski KJ, et al. (2006) Mechanical properties of electrospun fibrinogen structures. *Acta Biomater* 2:19-28.
35. McManus MC, Boland ED, Simpson DG, Barnes CP, Bowlin GL (2007) Electrospun fibrinogen: Feasibility as a tissue engineering scaffold in a rat cell culture model. *J. Biomed Mater Res A* 81: 299-309.
36. Wnek GE, Marcus Carr E, David Simpson G, Gary Bowlin L (2003) Electrospinning of nanofiber fibrinogen structures. *Nano Letters* 3: 213-216.
37. Boland ED, Matthews JA, Pawlowski KJ, Simpson DG, Wnek GE, et al. (2004) Electrospinning collagen and elastin: Preliminary vascular tissue engineering. *Frontiers In Bioscience* 9: p1422-1432.
38. Bashur CA, Dahlgren LA, Goldstein AS (2006) Effect of fiber diameter and orientation on fibroblast morphology and proliferation on electrospun poly(D,L-lactic-co-glycolic acid) meshes. *Biomaterials* 27: 5681-5688.
39. Sell SA, McClure MJ, Barnes CP, Knapp DC, Walpoth BH, et al. (2006) Electrospun polydioxanone-elastin blends: potential for bioresorbable vascular grafts. *Biomedical Materials* 1: 72-80.
40. Boland ED, Coleman BD, Barnes CP, Simpson DG, Wnek GE, et al. (2005) Electrospinning polydioxanone for biomedical applications. *Acta Biomaterialia* 1: 115-123.
41. Sell SA, Wolfe PS, Ericksen JJ, Simpson DG, Bowlin GL (2011) Incorporating Platelet-Rich Plasma into Electrospun Scaffolds for Tissue Engineering Applications. *Tissue Engineering* In review.
42. Boland ED, Telemeco TA, Simpson DG, Wnek GE, Bowlin GL (2004) Utilizing acid pretreatment and electrospinning to improve biocompatibility of poly(glycolic acid) for tissue engineering. *Journal of Biomedical Materials Research Part B: Applied Biomaterials* 71B: 144-152.
43. Francis MP, Sachs PC, Elmore LW, E Holt S (2010) Isolating adipose-derived mesenchymal stem cells from lipoaspirate blood and saline fraction. *Organogenesis* 6: 1-4.
44. Kevy SV and Jacobson MS (2004) Comparison of methods for point of care preparation of autologous platelet gel. *J Extra Corpor Technol* 36: 28-35.
45. Boland ED, Wnek GE, Simpson DG, Pawlowski KJ, Bowlin GL (2001) Tailoring tissue engineering scaffolds using electrostatic processing techniques: A study of poly(glycolic acid) electrospinning. *Journal of Macromolecular Science Part A: Pure and Applied Chemistry* A38: 1231-1243.
46. Moroni L, Licht R, de Boer J, de Wijn JR, van Blitterswijk CA (2006) Fiber diameter and texture of electrospun PEOT/PBT scaffolds influence human mesenchymal stem cell proliferation and morphology, and the release of incorporated compounds. *Biomaterials* 27: 4911-4922.
47. Xiao-Yu Sun, Nobles L R, Börner HG, Spontak RJ (2008) Field-Driven Surface Segregation of Biofunctional Species on Electrospun PMMA/PEO Microfibers. *Macromolecular Rapid Communications*, 29: 1455-1460.
48. Chiu JB, Liu C, Hsiao BS, Chu B, Hadjiargyrou M (2007) Functionalization of poly(L-lactide) nanofibrous scaffolds with bioactive collagen molecules. *Journal of Biomedical Materials Research* 83A: 1117-1127.
49. Sun XY, Shankar R, Börner HG, GhoshTK, SpontakRJ (2007) Field-Driven Biofunctionalization of Polymer Fiber Surfaces during Electrospinning. *Advanced Materials* 19: 87-91.
50. McClure MJ, Sell SA, Barnes CP, Bowen WC, Bowlin GL (2008) Cross-linking electrospun polydioxanone-soluble elastin blends: Material characterization. *Journal of Engineered Fibers and Fabrics* 3: 1-10.
51. McDonagh J, Messel H, McDonagh RP Jr, Murano G, Blombäck B (1972) Molecular Weight Analysis of Fibrinogen and Fibrin Chains by an Improved Sodium Dodecyl Sulfate Gel Electrophoresis Method. *Biochimica et Biophysica Acta* 257: 135-142.
52. Hirayama K Akashi S, Furuya M, Fukuhara K (1990) Rapid Confirmation and Revision of the Primary Structure of Bovine Serum Albumin by ESIMS and FRIT-FAB LC/MS. *Biochemical and Biophysical Research Communications* 173: 639-646.
53. Feng R, Konishi Y, Bell AW (1991) High Accuracy Molecular Weight Determination and Variation Characterization of Proteins Up To 80 ku by Lonspray Mass Spectrometry. *Journal of American Society of Mass Spectrometry* 2: 387-401.
54. Aliberti G, Proietta M, Pulignano I, Del Porto F, Tammeo A, et al. (2010) Association between fibrinogen plasma levels and platelet counts in an outpatient population and in patients with coronary heart disease. *Blood Coagulation and Fibrinolysis* 21: 216-220.
55. Man D, Plosker H, Winland-Brown JE (2001) The Use of Autologous Platelet-Rich Plasma (Platelet Gel) and Autologous Platelet-Poor Plasma (Fibrin Glue) in Cosmetic Surgery. *Plastic and Reconstructive Surgery* 107: 229-237.
56. Barnes CP, Smith MJ, Bowlin GL, Sell SA, Tang T, et al. (2006) Feasibility of electrospinning the globular proteins hemoglobin and myoglobin. *Journal of Engineered Fibers and Fabrics* 1: 16-29.